arXiv:1609.08378v1 [cond-mat.soft] 27 Sep 2016

Network formation and gelation in Telechelic Star Polymers

Indrajit Wadgaonkar[1], Apratim Chatterji[2*]
1 *Flat I-308, Nakshatra I-Land, Moshi-Alandi Road, Pune-412105.*
2 *IISER-Pune, 900 NCL Innovation Park, Dr. Homi Bhaba Road, Pune-411008, India.*
(Dated: September 28, 2016)

We investigate the efficiency of gelation and network formation in telechelic star polymer melt, where the tips of polymer arms are dipoles while rest of the monomers are uncharged. Our work is motivated by the experimental observations [1], in which rheological studies of telechelic star polymers of poly-(L-actide), a bio-degradable polymer, showed a drastic increase in elastic properties (up to 2000 times) compared to corresponding star polymers without the telechelic arm ends. In contrast to previous studies, we avoid using effective attractive Lennard Jones potentials or dipolar potentials to model telechelic interactions. Instead we use explicit Coulomb positive and negative charges at the tip of polymer-arms of our bead-spring model of star polymers. By our simulations we show that the dipoles at the tip of star arms aggregate together to form clusters of dipoles. Each cluster has contribution from several stars, and in turn each star contributes to several clusters. Thus the entire polymer melt forms a connected network. Network forming tendencies decrease with decrease of the value of the effective charge constituting the dipole: this can be experimentally realized by choosing a different ionomer for the star tip. We systematically varied the value of dipole charges, the fraction of star-arms with dipoles at the tip and the length of the arms. The choice of explicit charges in our calculations enables us to make better quantitative predictions about the onset of gelation, moreover we get qualitatively distinct results about structural organization of dipoles within a dipole-cluster.

PACS numbers: 82.30Nr,82.35.Pq,82.20.Wt

I. INTRODUCTION

The need for designable and tunable biodegradable polymers cannot be overemphasized in the present scenario. Often the synthesized biodegradable polymers do not have the required properties, and then suitable modifications have to be implemented on the polymer chains to get the desired properties [2–5]. One such example of a synthesized polymer melt has been poly-(L-lactide), a biodegradable and bio-renewable polymer [1]. But unfortunately, the melt strength, the maximum tension that can be applied to the melt without breaking, of poly-lactide is quite low which makes it unsuitable for extrusion to thin plastic sheets or pipes or bags. Melt strength, an indication of the value of the elastic response modulus $G^{'}$ of the melt, increases with the decrease of the viscosity η of the melt. It is obvious without increase of $G^{'}$, poly-(L-lactide) cannot be used as a replacement for standard polymeric products available for use.

Using some ingenious chemistry, $1-4\%$ of the L-lactide monomers were replaced by another suitable ionic group [1], the elastic modulus of poly-(L-lactide) was increased by a factor of 2000 times. The question is how and why is that possible? In this paper we investigate the microscopic basis of this huge increase in the elastic modulus using simple bead spring models of polymers and properties of telechelic polymers. We quantify limits to which the experimentally suggested method of increasing the $G^{'}$ [1] or the melt strength can be explored and extended.

*Electronic address: apratim@iiserpune.ac.in

As per experimental evidences [1], suitably polymerized L-lactic acid (PLA) is a star polymer with 6 arms with 25 lactic acid monomers per arm. Thus a PLA star has 150 monomers, and the elastic and viscous response functions, $G^{'}$ and $G^{''}$ were measured to be 1 and 10 pascals, respectively, in the newtonian rheology regime. When the monomers of the 6 arms of stars polymers were suitably substituted to have $Na^{+}-COO^{-}$ ionomers only at the tip of star arms, the $G^{'}$ increased to 2000 pascals and the $G^{''}$ to 500 pascals. When further rheological experiments with different number of ionomers per star were performed, the elastic response increased by a factor varying from 10 to 2000 times, as the number of ionic end groups per star f was varied. Experimental control can be achieved such that the star melt has on an average just 2 or 3 or 4 ionic end groups per star. The reader is encouraged to appreciate that the change in composition is in just 2,3 or 6 monomers out of 150 monomers in a star and just at arm-tips, but the increase in elastic and viscous response is huge.

There are been previous work as well on linear and star polymers with different functionalized end groups at the tip of a polymer chains [6, 7], and they observe an increase of visco-elastic response of polymers depending on the nature of ions and architecture of polymers. The general expectation and understanding is that the ionomers form clusters of telechelic sections of chains, and this ends up in the physical gelation of polymers chains [7]. This could lead to formation of star polymers starting from telechelic linear polymers, or induce conformational changes in individual star-polymers [8, 9, 11] or in the structural rearrangements in the large scale organization of stars [10, 12]. Other theoretical/computational studies

with telechelic chains have focussed on finding the sol-gel phase diagram of telechelic polymers in dilute polymeric systems or the dynamical properties of associating polymers due to telechelic ends [13–15] including change in glass transition temperature [19]. But nearly all studies telechelic polymers, also known as end-functionalized polymers in literature [16], model the attraction between telechelic ends by an attractive Lennard Jones potential with a cut off at a suitable distance. Moreover, most of the the theoretical studies of telechelic stars stick to the dilute limit. Previous experimental studies using poly-(L-lactic acid) ionomers had considered linear polymers and observed the increase in glass transition T_g due to the presence of ionomers [17, 18].

In a departure from previous computational studies, in our study we focus on a bead-spring model of a star polymer *melt* with telechelic ends modelled as dipoles with *explicit charges* instead of effective attractive potentials. The usually used effective attractive potentials (e.g. Lennard Jones) used to model telechelic properties provide attraction at short length scales, on the contrary the Coulomb interaction acts between monomers far separated in space. We consider stars with 6 arms, and 25 monomers per arm in tune with the experiments [1] which motivated this investigation. The last two monomers of the star arms are replaced by a postively and negatively charged monomer, such that we have a dipole which in turn attempts to model the presence of Na^+ and COO^- ionomers at the arms tips of poly-(L-lactide) stars. We carry out Molecular dynamics simulation of such star ionomers, and vary the values of effective charges $\pm qe$ at the star polymer ends, where q is a fraction < 1 and e is the electronic charge. Variation of the value of q at the star tips would experimentally correspond to substituting different ionomers at the tip of star arms, as has been considered in a previous study [7].

We establish at which values of q do multiple dipoles aggregate together to form dipole-clusters overcoming thermal effects. These dipole clusters are multiply connected to many stars, and each star contributes to many dipole clusters thereby forming a gel-like interconnected network of polymers. If one has just 2 or 3 dipoles per star, then obviously the dipole clusters formed are smaller and then one has macromolecular assemblies instead of system-spanning percolating networks of stars connected through dipole clusters. We do not compute dynamical quantities like viscosity or $G^{'}$ in our simulations as the calculations are too expensive, instead we focus on morphological quantities and deduce that the relaxation times will increase per microscropic structure changes.

We emphasize that in contrast to previous studies of dipolar fluids [20–25], where the authors have used the dipolar potential as a $1/r^2$ potential valid at large distances away from the dipoles, we use explicit charges $\pm qe$ to model the dipoles. In our work the interaction energy between the dipoles is thereby calculated using explicit Coulomb potential between each pair of charges. This is necessary because the dipolar monomer pairs can be atomistically close to each other where the multipole Taylor expansion is not even valid. As a consequence, the structure and and organization of dipoles in a dipole cluster in our studies is different from what has been found in previous investigations of dipolar fluids [23–25] when the interaction potential between dipoles is modelled as $1/r^2$ potential.

The rest of the paper is organized as usual, the next section consists a detailed description of our model where we have taken extra effort to connect with experimental numbers; we also state when we deviate from experimental conditions. We do not use the effective charges q for Na^+ and COO^-, instead vary it as a parameter. In section III, we present our results, and finally we conclude in section IV with a discussion and future outlook.

II. METHOD

Molecular dynamics simulations of PLA star ionomers were performed using a bead spring model of polymers. Each lactic acid monomer was modeled as a spherical bead connected by harmonic springs to the neighbouring monomers. The spring interaction between two neighbouring monomers are given by

$$V_{spring} = \kappa(x - \ell_0)^2 \tag{1}$$

where ℓ_0 is the mean distance between monomers and $\ell_0 = 1$ sets the length scale of the simulation. Each star polymer has 6 arms and there are $L = 25$ lactic acid monomers per star. The six linear polymer arms are attached to a central sphere by

$$V_{sphere} = \kappa_s(x - \ell_0^{sph})^2 \tag{2}$$

where $\kappa_s = \kappa = 1000 k_B T$ and $\ell_0^{sph} = 2\ell_0$. We set $k_B T = 1$ and all other energies are measured in units of $k_B T$, e.g., $\kappa = 1000 k_B T$. A very high value of $\kappa = 1000 k_B T$ is chosen to render the polymer arm to be inextensible chain. Excluded volume interaction between the beads are incorporated by a suitably shifted purely repulsive Lennard Jones interaction truncated at a distance $r_c = 2^{1/6}\sigma$, where $\sigma = 0.8\ell_0$ is the diameter of the monomeric beads. The excluded volume radius of the central sphere is $\ell_0^{sph} - 0.5\sigma = 1.6\ell_0$. We have chosen a large central sphere so that we can add more number of arms around central sphere in future studies as in [26–28]. The mass M of each monomer is set as $M = 1$. Giving suitable values to $k_B T$, M and ℓ_0, we can calculate suitable values to quantitites of interest like κ, the calculated average energy of the system or unit of time $\tau = \sqrt{(M\ell_0^2/k_B T)}$. For example, setting $T = 300$K, $\ell_0 = 1nm$ and $M = 15 \times 10^{-23} kg$ for a lactic acid monomer, we get $\tau = 0.2$ nanoseconds. But for purpose of simulation, we set $k_B T = 1, M = 1, \ell_0 = 1$ and measure all other quantities in these units.

The presence of Na^+ and COO^- at the end of the arms of the PLA star results in an effective dipole at the tip

of every polymer arm; these dipoles in turn interact and attract/repel each other depending upon their relative orientation. We do not model dipolar interaction by the $\frac{1}{r^2}$ dipolar potential as this approximation breaks down at distances when the dipoles are close to each other, instead we use the Coulomb potential between each pair of charges. We consider the 25-th and 24-th monomer at the tip of each arm to have a charge of $+qe$ and $-qe$, respectively, where $q < 1$ is a fraction and e is the electronic charge. In our simulations, we can set all the 6 arms to have dipoles at the tip. In this case, the number f of dipoles per star is $f = 6$. Alternatively, we can choose to have a system where only 2 or 3 out of 6 arms have charges at the tips of polymer arms, which then corresponds to $f = 2$ or $f = 3$, respectively. To compare our simulations results to experiments, ideally we would also need to know the effective charges on the Na^+ or COO^- ions at the end of the PLA arm. Since we do not know the effective charge qe at each ionomer, we use 4 different values of effective charges qe and analyze the network formation between stars for each value of q.

To put numbers into perspective, two isolated electronic charges $+e$ and $-e$ at a distance of $\ell_0 = 1$ nm from each other have a Coulomb energy $E_c(e, 1nm) \approx 61 k_B T_1$ for $T_1 = 300K$. For our simulations we use 4 different values of effective charge with appropriate value of q such that $R = E_c(qe, \ell_0)/k_B T$ has values $R = 5, 10, 20, 40$, respectively. Since $E_c(qe, 1nm) = q^2 61 k_B T$, the value of R can also be expressed as $R = 61q^2$, and as before R remains dimensionless. We then study how R affects structural arrangement of stars and dipoles at the microscopic length-scale. The calculation of Coulomb forces in a finite box with periodic boundary conditions (PBC) would necessitate the use of Ewald summation techniques or alternatively P^3M (particle-particle particle mesh), especially since electrostatic interactions have long ranged $\sim 1/r$ potentials. We use LAMMPS simulation package [29] with a cubic box. LAMMPS has inbuilt P^3M [30, 31] implemented which we use to calculate Coulomb interaction between dipoles at tips of arms.

For our simulations we maintain our star polymer melt densities close to that used in experiments [1]. The PLA melt density of stars in 1.06 gm/cm^3 and molecular weight of stars is 10000 gm/mol. Thereby 1cm^3 contains $\sim 10^{-4}$ moles of PLA stars $\sim 6 \times 10^{19}$ stars, and thus we calculate that one star occupies $16.7 \times 10^{-27} m^3$. If we assume that the star is a sphere occupying the specified volume, we can estimate the approximate value of star-radius to be ≈ 16 Å. To the first approximation, the radius of the star is equal to the radius of gyration r_G of a polymer arm, thus $r_G == L^{0.6} l_0^e/\sqrt{6} = 16\mathring{A}$, where $L = 25$ is the number of monomers in a star arm. So the effective bond length ℓ_0^e is 5.6 Å, which is nearly half the length $\ell_0 = 1nm$ used to estimate R in our simulations, So a simulation box of $50 \times 50 \times 50(\ell_0^e)^3$ should have ~ 1300 star polymers.

For our simulations we deviate from exact experimental values to study a less dense system. For computational ease, we take 350 stars in a cubic box of volume $L^3_{box} = 50 \times 50 \times 50 \ell_0^3$, and carry out our simulations to investigate the equilibrium structure of the stars and the resultant clustering of dipoles as a function of R, f for $L = 25$ and $L = 50$. Different values of R correspond to different values of partial charge qe on the charges constituting the dipoles at polymer arm tips. For our simulations we start with the equilibrated configuration of a single star polymer (without dipoles at arm tips) in a simulation box, then 349 copies of this equlibrated configuration are placed and packed in a lattice within a $50 \times 50 \times 50 \ell_0^3$ simulation box and then equilibrated for 10^5 iterations using Molecular dynamics (MD) to create a melt of star polymers. Then dipolar charges at the tips of arms are switched on and the system is further equilibrated (10^5 iterations) to have a melt of star polymers with dipoles at arm tips. During equilibration we use a thermostat which rescales the velocities every 20 iterations to maintain temperature $k_B T = 1$. Integration time step was chosen to be $\delta t = 0.001\sqrt{(M\ell_0^2/k_B T)} = 0.001\tau$. Independent runs were given to cross-check that the star ionomer melt reached the same equilibrium energy and structural arrangement of stars. Note that the number of arms per star always remains fixed at 6; when $f = 2$ it implies that only 2 out of 6 arms have dipoles at the tips of arms while 4 star-arms remain uncharged.

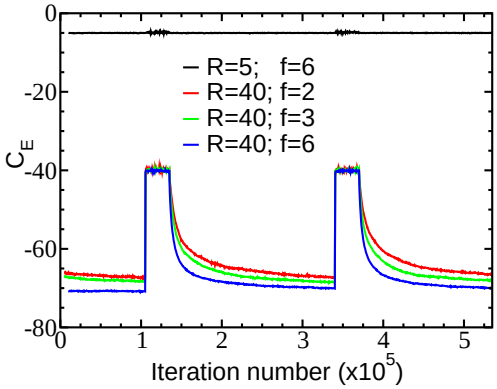

FIG. 1: The average Coulomb energy per dipole C_E versus the number of iterations over 2 heating and cooling cycles starting just after the first 10^5 iterations of an equilibrated system. The system is heated to $50 k_B T$ for 30000 iterations, and then allowed to equilibrate for next 10^5 iterations at $1 k_B T$, and we then collect statistical data for the next 10^5 iterations. Data is shown for $R = 40$ and $R = 5$. The fluctuations in C_E is more at higher temperatures.

Because a melt of gel-like polymers is a dense system with long relaxation times, we have to ensure that the statistical quantitities that we measure are not the properties of a configuration stuck in a initial condition dependent free energy minimum. To that end, after completion of equilibration and collecting statistical data for the initial 10^5 iterations, we heat the system to $T_{50} = 50T$ (where $k_B T = 1$) and keep the system at high temperatures for 30000 iterations, such that the system gets

thermalized at high T. Then the system is cooled down back to T, allowed to equilibrate for 1.05×10^5 iterations. We checked that a completely different and statistically independent configuration and dipole cluster is formed after the cooling. Then statistical data is collected over the next 10^5 iterations, every 200 steps before heating it again to $50k_BT$. This heating and cooling cycle is shown in Fig.1 where the energy per dipole C_E is shown for different values of f at $R = 40$ for $L = 25$ stars. The value of C_E shoots up when temperature is T_{50}, but then relaxes to equilibrium in around 10^5 iterations once the temperature is reset to T.

The heating to $T_{50} = 50T$ and cooling was carried out 4 times, the statistical data was compared and seen to be equivalent in each of 5 sets of runs over which data was collected. For example, the average number of clusters in the box for the system $R = 40, f = 6$ and $L = 25$ in the 5 individual runs were $217, 210, 216, 198$ and 202, respectively. Similarly, the average number of clusters for the system $R = 5, f = 6$ and $L = 25$ in the 5 set of runs were $1701, 1774, 1775, 1779$ and 1774, respectively. We also compared the mean size of dipole-aggregates formed across 5 runs and found them to be comparable within statistical fluctuations. The data that we present in the results section is a statistical average of the initial run and 4 runs after heating-cooling and equilibration. Though 30000 iterations at $50k_BT$ might not result in the diffusion of stars over length scales comparable to the diameter of the stars, it is enough to break any dipole clusters and make the arms move considerably in phase space. To that end, after cooling the dipole cluster configuration is completely independent of previous configuration.

In Fig.1, we show the average Coulomb energy per dipole C_E versus number of iterations with $R = 40$ for 3 different values of f (and hence different dipoles densities), as well as for $R = 5$ for $f = 6$. After the initial equilibration of the system at $k_BT = 1$, the Coulomb energy per dipole C_E for $R = 40, f = 2$ system relaxes to $\approx 65k_BT$. This is lower than the energy of 2 charges kept at a unit distance from each other, which is $40k_BT$. Presumably dipoles attract and come together to form dipole aggregates and each charge interacts with many other charges. But C_E goes up to $40k_BT$ when the temperature is increased to T_{50} (such $T_{50}/T = 50$) at around 10^5 iterations. We checked thermal energy at T_{50} disintegrates any dipole clusters. For $f = 3$ the value of $C_E(T)$ is slightly lower than that for $f = 2$ stars, and for $f = 6$ with higher density of charges $C_E \approx 70k_BT$. The value of C_E/k_BT goes nearly to 40 at temperature T_{50} for all values of f. This is not difficult to understand, as the thermally averaged effective interaction between freely rotating dipoles become a effective short range attractive $1/r^6$ interaction as is well discussed in the classic book by Israelachvili [32].

The primary message from Fig.1 is that when the temperature is reduced back to T_1 from T_{50}, the Coulomb energy relaxes back to the same lower value in approximately 10^5 iterations for each value of f. This assures us the system is equilibrated and we can start collecting data for statistical averages after this cooling step till the system temperature is again hiked to T_{50}. We also checked the value of C_E for $R = 5$ for $f = 6$, the Coulomb interaction energy is nearly 5 even at $k_BT = 1$; though there is more energy fluctuations when the temperature is hiked to T_{50}. This would imply the organization of dipoles at low and high temperature is similar and thermal energies overwhelms Coumlomb correlations or clustering. Indeed we show later that for $R = 40$ we get clusters of dipoles, whereas for $R = 5$ most of the dipoles do not form aggregates with other dipoles.

III. RESULTS

In this section we discuss our measurements and conclusions regarding the structure formation in telechelic star polymers in some detail. We ask and quantify 4 primary questions:

1. Do the dipoles at the tip of star-polymer arms aggregate together to form clusters of dipoles? If yes, how big are the clusters?, i.e., How many dipoles are there in one cluster? If many clusters are formed, what is the distribution of the cluster sizes? These set of questions are analyzed and quantified in Figs. 3,4,5 and 6.

2. Do the dipoles of a particular cluster belong to a single star? Or does a dipole-cluster have contributions from the arms from different star polymers? If so, how many stars?

   A dipole cluster can behave as a node at which different star arms get attached and are held together due to dipolar attraction. If some of the clusters have more than (say) 6 or 10 dipoles (or more), and if most of the clusters have contributions from many stars, then each dipole-cluster connects up many star-polymers. Then the likely scenario is that all the stars arms in the system will form a percolating network connected by dipole clusters and the system would be akin to gel state of polymers. These set of questions are investigated using data presented in Fig. 7 and 8.

3. Reversing the previous question, how many different clusters does each star contribute to? Do all the different arms of a star contribute dipoles to different clusters. If yes, it would definitely help form a percolating network of stars or a macroscopic gel of multiply-connected stars. Each star arm would be connected to many different stars through a dipole cluster. Refer Figure 9,10 for discussions.

4. How would doubling the length of star arms help/hinder the cluster formation with dipoles ? A polymer arm could potentially explore more phase space and help forming bigger dipole clusters and help stars form networks.

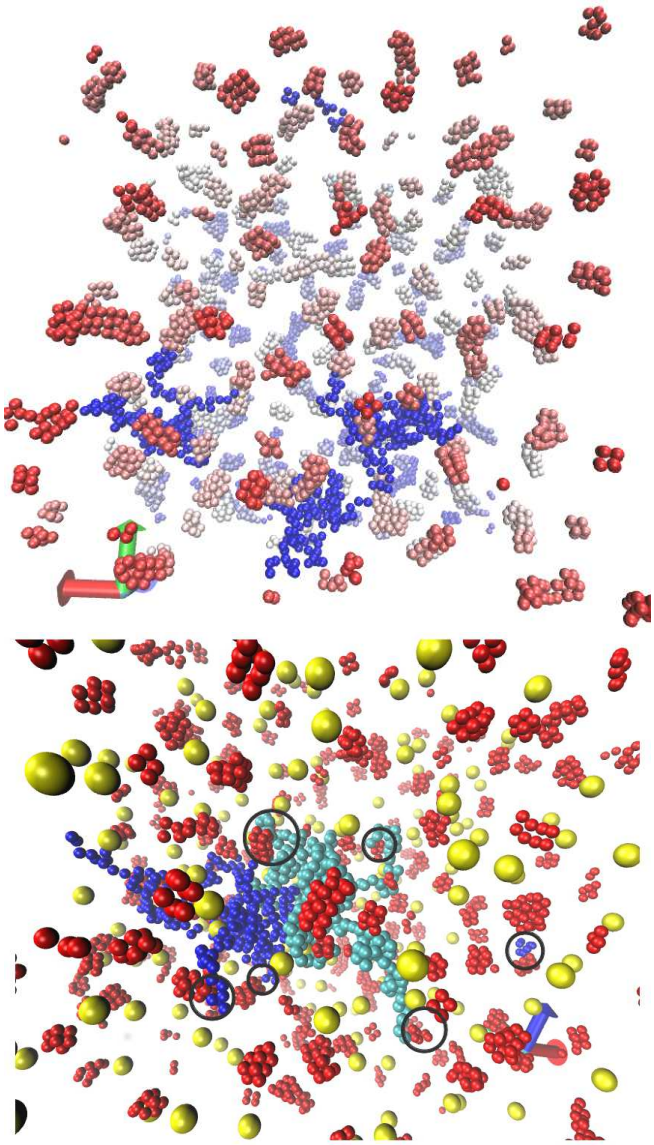

FIG. 2: Representative snapshots from our simulations of star polymers with 6 arms and $f = 6$ for $L = 25$ monomers in each arm (top figure) and $L = 50$ (bottom figure) at $R = 40$. Each arm has a dipole at the tip of arms: $f = 6$. We show uncharged monomers (small blue spheres) of only 3 stars (top) and 2 stars (bottom) out of the total stars present. All the charged monomers from each of the stars are shown as slightly bigger red spheres with color gradient in the direction pointing into the paper (top) but no color gradient in the bottom figure. Dipoles aggregate to form clusters, furthermore, different star arms connect to different clusters. This is clearly seen in top panel, but we have marked by circles in the bottom panel for the ease of reader. The star centers, shown as yellow big spheres in the bottom panel, are homogeneously distributed over the simulation box. In each panel, we see a few uncharged monomers of a star-arm isolated from the rest of star, this results from periodic boundary condition applied to the simulation box.

The primary quantities to vary are the effective charges qe constituting the dipoles thereby changing interaction energy between dipoles and the quantity f: the number of dipoles per star polymer. Instead of using fractional charge qe, we use quantity R such that we can directly compare the thermal energy k_BT and the electrostatic energy between 2 charges at a distance of ℓ_0 $(= 1nm)$ between them. We have also considered 2 values of L, the number of monomers in each arm of the star polymer: we considered $L = 25$ monomers per arm as was used in experiments [1] as well as $L = 50$ monomers. To compare results of $L = 25$ and $L = 50$ monomers per arm, we halve the number of stars to 175 stars in the simulation box for the $L = 50$ runs, thereby we keep the number of monomers fixed. For reference and clarity, we give the relevant dipole/monomer numbers in Table. I as L and f is varied. We keep the number of arms per star remains fixed at 6. The arms can rotate freely about the center, hence, it is not relevant to discuss which particlular arm has the dipoles when $f = 2$ and $f = 3$. For $f = 6$, of course, each arm of each star has a dipole at the arm-tip. In addition there are 350/175 central beads of diameter ℓ_0^{sph} for $L = 25/L = 50$ star systems, respectively.

In Fig.2, we show two snapshots from our simulations which show how star-arms contribute dipoles to different clusters. The top figure is for stars with $L = 25$ monomers per arm; the bottom figure is for stars with $L = 50$ with $f = 6$. We have plotted the monomers (blue small spheres) of only 3 and 2 representative star-polymers, respectively, out of the 350 stars present in the box for ease of visualization. All the dipoles from each of the arms of stars are shown in the snapshot to give the reader an idea of spatial and size distribution of dipole clusters. The dipoles are shown in red (slightly bigger spheres than monomers), the red spherical aggregates indicate clusters of dipoles formed. One sees that the dipoles arrange to form elongated aggregates. This is presumably to arrange the dipoles anti-parallel to each other with negative charge next to the positive charge and is in marked contrast to the chain like structures reported in [23–25] who use the dipolar approximation of the interaction potential. We have checked that for lower values of R, e.g. $R = 20, 10$ the dipoles cluster is shaped more like a globule rather than arranged in rod-like clusters. The snapshot at the bottom with 175 stars has half the number of dipoles than the snapshot at top. In bottom panel, we can see only part of the box as we have zoomed in on the part which has stars for better clarity. One can also visually analyze how the different arms contribute dipoles to dipole-clusters: in the bottom snapshot we have encircled 6 arms where different star-arms end up in different dipole clusters to help the reader. The bottom snapshot also shows the distribution of star centers (big yellow spheres), and one can infer that they are relatively uniformly distributed in the system and there is no aggregation of star-centers around big clusters of dipoles. The qualitative conclusions arrived at from the snapshot is quantified in the figures that follow.

Figure 3 quantifies the ideas presented in Fig.2 and shows the average of total number of dipole-clusters C_T

L	S_T = No. of Stars	f	N_D
25	350	6	2100
25	350	3	1050
25	350	2	700
50	175	6	1050
50	175	3	525
50	175	2	350

TABLE I: Table listing the number of dipoles in the simulation box for as L and f is varied. The total number of monomers always remains fixed at $L * f * S_T = 52500$. There are 175/350 central monomers if there are 175/350 stars in simulation box. Number of dipoles $N_D = f * S_T$.

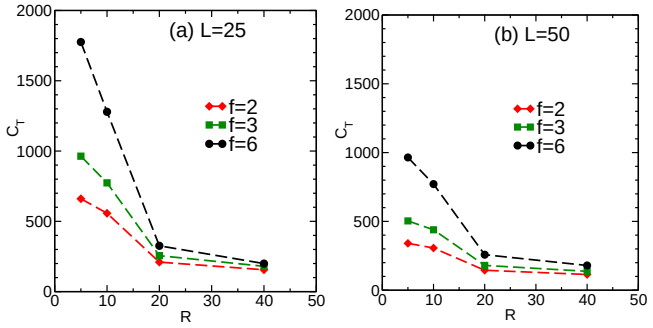

FIG. 3: Figure shows the average of total number of clusters C_T in the system versus R, for different values of f, the number of dipoles per star. Subplots (a) and (b) are for $L = 25$ and $L = 50$ with 350 and 175 stars in the simulation box, respectively. The quantity R is the ratio of energy $E(qe, 1nm)$ and k_BT, where $E(qe, 1nm)$ is the energy between two partial charges $\pm qe$ at a distance 1nm from each other. There are two distinct regimes: $(i)$for $R = 5$ or $R = 10$ the value of $C_T \sim N_D$, where N_D is the total number of dipoles in the system. This indicates that most clusters have just 1 dipoles. (ii) For $R = 20$ or $R = 40$, $C_T \ll N_D$, indicating the each cluster has a large number of dipoles aggregated together in a cluster. Data presented is over 4 rounds of heating and cooling cycles, and after each cycle a statistically independent set of clusters are formed. Data has not been normalized by N_D, since this data will be used later for analysis.

as a function of R for different values of f. We define 2 dipoles to belong to the same cluster if the distance between the center of 2 charged monomers belonging to different stars arms is less than 1.2σ. A cluster of size 1 indicates there is only a dipole in the cluster implying that the dipole has not formed an aggregate with another dipole. Data presented in Fig. 3 is for $L = 25$ and $L = 50$ monomers per arm in subplot (a) and (b), respectively. For $R = 5$ and $R = 10$, the total number of clusters C_T for all fs is only slightly less than the total number of dipoles N_D in each case (refer TableI) implying that most dipoles are isolated and free in space. Most of the cluster are essentially a $1-$dipole cluster, and very few clusters have 2 dipoles.

In contrast, for $R = 20$ and $R = 40$, the average number of clusters C_T in the box are much smaller than N_D, indicating that majority of dipoles are in clusters and each cluster has multiple dipoles. Refer Table I for the values of N_D. The value of C_T calculated using the data of Fig.4 and 5: $C_T = \sum C \times n_c$, where the summation is over the number of dipoles C in a cluster. The average number of clusters containing C dipoles is denoted by n_c: n_c versus C data is discussed in the next paragraph. Note that the number of clusters keeps fluctuating as dipoles aggregate to form clusters and then break apart due to thermal energy. In addition, when the system is heated to $50k_BT$, every cluster disintegrates completely, and a new distribution of dipole-clusters is formed once the system is cooled down. Thus n_c, and thereby C_T is a statistically averaged quantity. In the data presented in subplot (b) for $L = 50$, we again observe that $C_T/N_D \approx 1$ for $R = 5, 10$, whereas as one increases $R = 20, 40$ there is aggregation of dipoles to form larger clusters.

Figure4 shows the distribution of the number of dipole-clusters n_c for a particular size of the cluster C; the size C of dipole-cluster is calculated by the number of dipoles in the particular cluster. For $R = 40$ and $f = 6$, all the dipoles at the end of star-arms have aggregated to form clusters: there are no clusters of size 1: refer subplot 4(a). In Fig.4a, there are on an average 5 large clusters containing $C = 15$ dipoles in each cluster. Clusters containing 16/17/18 dipoles occur in the box with similar frequency. Even bigger clusters with more than 20 dipoles per cluster are seen though with less frequency for $R = 40$. Clusters with $6 - 10$ dipoles per clusters are found with the highest frequency as shown in the peak of the distribution. For lower values of $f = 3$ and $f = 2$ dipoles per star, the dipole density is lower in the box, and the peak of the distribution shifts to lower values of cluster size. In these cases, one sees large number of clusters with just 4 or 5 dipoles in a cluster. It is difficult to confirm if larger aggregates will form over much longer time scale of simulations, but we expect our present result to hold true. This is because diffusion of individual stars will be hindered because different arms of stars are in different clusters (as we show later) with relatively high values of Coulomb energy C_E/k_BT per dipole. Furthermore, large aggregates of dipoles with 25 (say) dipoles or more per cluster for $f = 2, f = 3$ will also result in local increase in density of the stars connected to the cluster, i.e, spatially inhomogeneous monomer density.

In figure 4(b), for $R = 20$ with $f = 6$, one observes that relatively smaller clusters are formed compared to when $R = 40$ and the peak of distribution has shifted to lower values of C. One concludes that there is lesser effective attraction between the dipoles to form large clusters and thermal energy destabilizes clusters with 20 or more dipoles per cluster. The peak of the distribution for $f = 6, 3, 2$ all lie at around 2 dipoles per cluster. However, for $f = 6$, there are more than 10 clusters each of size $10, 11, 12$, i.e. $n_C > 10$ for $C = 10, 11, 12$ each; so actually a large fraction of the dipoles can be expected to reside in clusters of size ≥ 10. The fraction of total dipoles which are in clusters of size C are plotted in Fig.

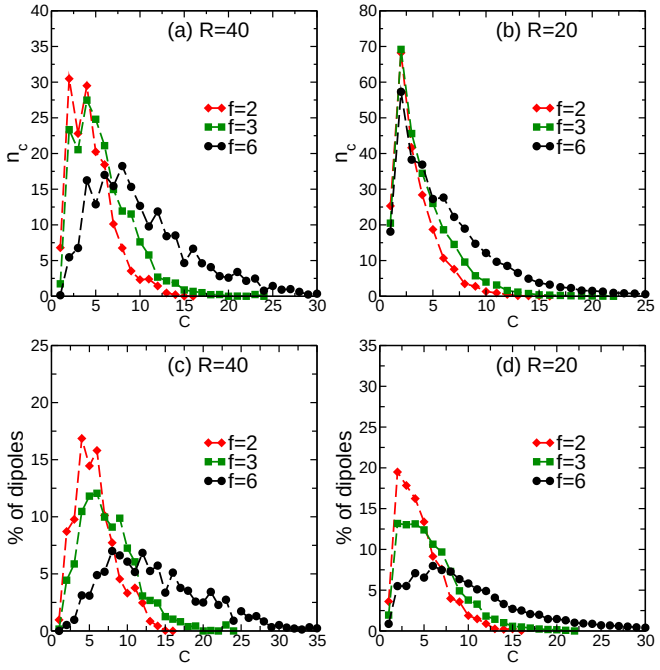

FIG. 4: The plots (a),(b) shows the distribution of the average number of clusters n_c of cluster size C for $R = 40$ and $R = 20$. The quantity C is the number of dipoles in a cluster. The number of dipoles at tip of arms in a 6 arm star polymer is denoted by symbol f, and we show data for different values of f for the number of monomers per star-arm $L = 25$. There are 350 stars in the simulation box. Subplots (c) and (d) show the percentage of dipoles which are to be found in clusters of size C for the corresponding set of parameters of (a) and (b) respectively. We have not suitably normalized the y axis for reasons given in the text.

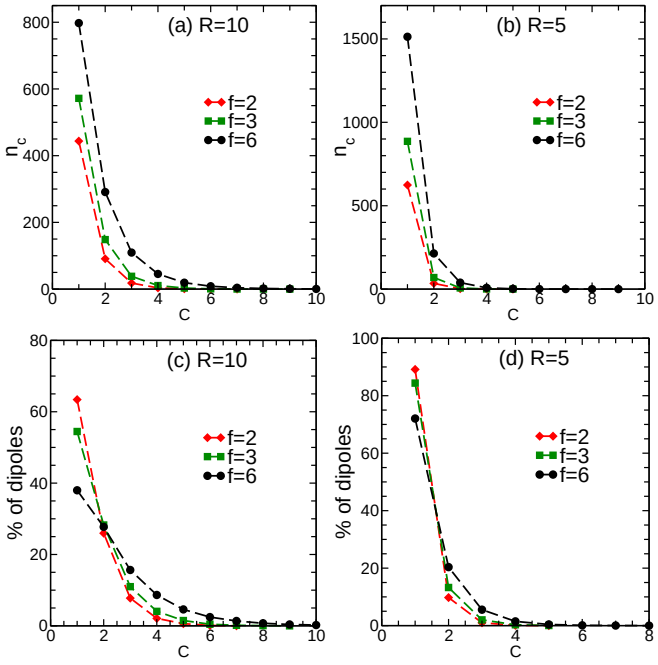

FIG. 5: The plots (a),(b) shows the distribution of the average number of clusters n_c versus the cluster size C for lower values of R, viz., $R = 10$ and $R = 5$ with different values of f. In contrast to Fig. 4, dipoles with $R = 10$ or $R = 5$ form very small aggregates with just one or two dipoles per cluster, i.e. the distribution is sharply peaked at $C = 1$ and $C = 2$. There are 350 stars in the box with $L = 25$ monomer per arm. Subplots (c) and (d) show the percentage of total number of dipoles which are observed in clusters of size C. We have not suitably normalized the y axis for reasons given in the text.

4c and 4d for $R = 40$ and $R = 20$. There are also a few large clusters (with $C > 10$) for $R = 20$, so actually around 45% of the dipoles are in clusters with $C \geq 10$ for $R = 20$ with $f = 6$. For $f = 2$ and $f = 3$ cases, the number of clusters with $C \geq 10$ decreases along with the fraction of dipoles in such clusters. This is obviously due to fewer number of dipoles present in the system for $f = 2, f = 3$. But still, independent of the value of f, at least 50% of the dipoles are in clusters with 6 or more dipoles for $R = 40, 20$. This also implies that 50% of the total number of stars arms contribute dipoles to clusters of size $C \geq 6$.

In Figures 4a and b, we do not normalize the y-axis by either the total number of dipoles N_D or by the average of total number of clusters C_T. The reason is that the total number of clusters is not a conserved quantity and does change due the course of the run. The total number of dipoles does remain fixed at $N_D = 2100, 1050$ or 700 for $f = 6, 3$ or $f = 2$, respectively, but then if the y-axis get divided by N_D, one looses the estimate of the number of clusters, especially for $f = 6$ where $n_c << N_D$.

The cluster size distribution is very different when $R = 10$ and $R = 5$, refer (a) and (b) of Fig. 5. The attraction between dipoles is hardly enough to bring dipoles together to form big aggregates, i.e., a cluster with more than 6 dipoles ($C > 6$, say) in a cluster. Most dipoles are free in space, a small number form dimers due to Coulomb attraction: thus entropy wins over Coulomb attraction between dipoles. For $R = 10$, there are more than 70% of dipoles in clusters which contain a single dipole or two dipoles ($C = 1$ or $C = 2$) for $f = 6$. The percentage of dipoles in a cluster with $C = 1$ increases for $f = 3$ and $f = 2$: refer Fig.5(c). In Fig.5d, we see that for $R = 5$ and $f = 6$, less than 10% of all dipoles form dipole-trimers or bigger clusters. This percentage reduces to nearly zero for $C = 3$ (or more) dipoles per cluster when $f = 2$ or $f = 3$.

These observations leads to the question that if the star polymers have longer arms, would that help forming bigger clusters of dipoles especially for $f = 2, f = 3$. One can imagine that different star-centers could be spread out in space and yet with the advantage of longer star arms and hence more reach, the dipoles could aggregate to form bigger clusters than when $L = 25$. As mentioned before, we do simulations with 175 stars with 6 arms each, but with 50 monomers per arm, i.e. $L = 50$ and compare it with the $L = 25$ data. The distribution of cluster sizes n_C versus C is presented in Fig.6 for different values of R and f. The number of monomers remain the same but

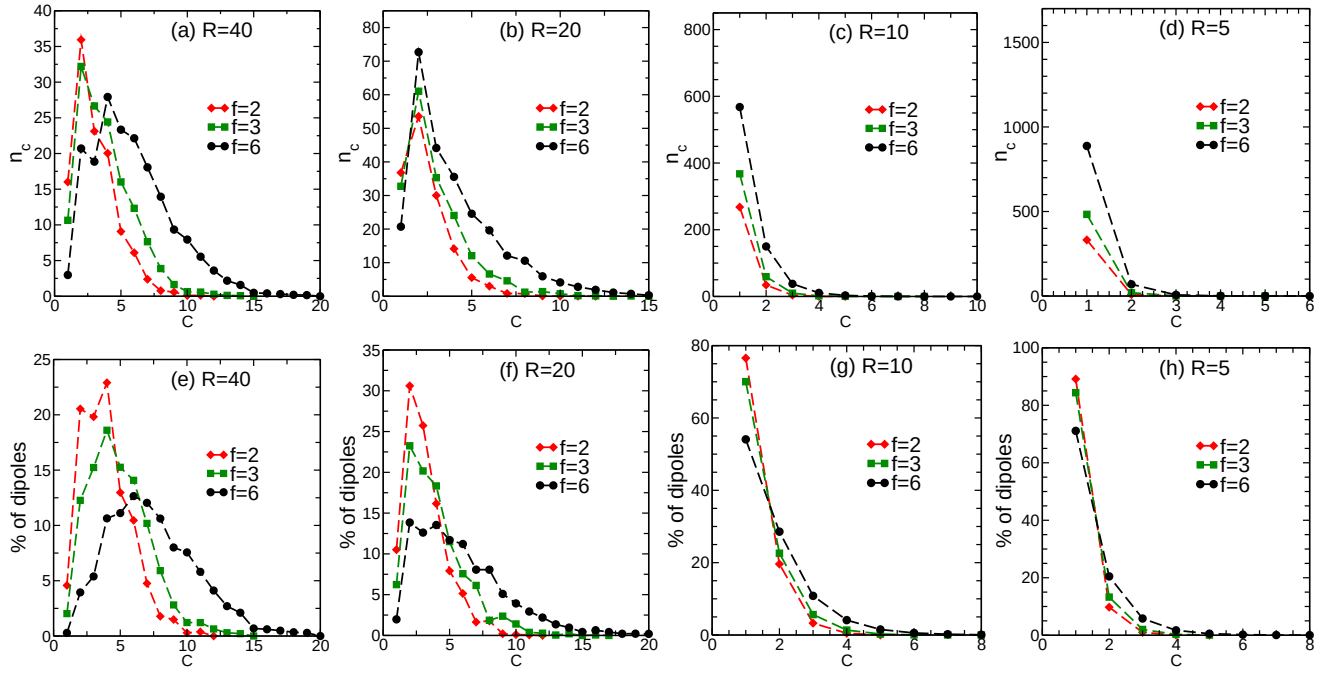

FIG. 6: The plots (a),(b),(c) and (d) shows the distribution of the average number of clusters n_c versus the cluster size C, for stars with $L = 50$ and 175 stars in the simulation box for $R = 40, 20, 10, 5$, respectively. The quantity n_C is the average number of clusters in the simulation box with C dipoles in a cluster. The figures at bottom (e),(f),(g),(h) show the percentage of total number of dipoles which are found in clusters of size C, so that we can estimate what fraction of dipoles are found in big/small clusters.

the number of dipoles at arm tips is halved, such that $N_D = 1050$. So data for simulations of $L = 50, f = 6$ system could be compared with $L = 25, f = 3$ data as they have the same dipole-density.

On comparison of Fig.6 with Fig.4 and Fig.5 we observe that the data for size distribution of clusters, i.e. n_C versus C are nearly the same for 2 systems with 2 different length of arms, but with identical N_D! For example, comparison of n_C vs. C of stars of length $L = 25$ with $f = 3$ and stars of length $L = 50$ with $f = 6$ shows that they are nearly identical, that too for each value of R. It implies that the doubling the length of polymer arms has no effect on the cluster size-distribution of dipoles, and cluster size distribution is decided primarily by the R value and the number density of dipoles in the box. Similar consistent behaviour can be observed if we compare cases $f = 2, L = 25$ and $f = 3, L = 50$ though the number density of dipoles is not exactly the same in these two cases. The fraction of dipoles to be found in clusters of size C are shown in figure 6e,f,g,h for $R = 40, 20, 10$ and 5, respectively.

In general, we make the following observations about the $L = 50$ system:

• For $R = 5$, 90% of dipoles with $f = 2$ stars and nearly 80% of dipoles of stars with $f = 6$ are isolated single dipoles. This is seen from the data at $C = 1$ in Fig.6d,h.

• As R value is increased from $R = 5$, the dipolar attraction between dipoles increases to gradually overcome the thermal effects. At $R = 20$ with $f = 6$, more than 50% of the dipoles are in clusters of size $C \geq 5$: refer Fig.6f. The peak of the size distribution data in Fig.6b is at $C = 2$, but still more than a third of the total number of clusters ($C_T \approx 240$, refer Fig.3b) are clusters with $C \geq 5$. Thus one could expect a large fraction of star-arms to be inter-linked by dipole clusters and the system could be in a gel state, if a cluster gets dipole contributions from different stars.

• For $R = 20$ with $f = 3$, the average number of clusters in the system is $C_T \approx 200$ (refer Fig.3b), and only one-fifth of dipoles (and only 1/8 of the clusters) have the number of dipoles in cluster of size $C \geq 5$.

• For $R = 40$ with stars with $f = 6$, nearly 65% of dipoles are in clusters with size $C \geq 5$, moreover, 50% of the total number of clusters have 5 or more dipoles. These fractions obviously are lower when $f = 2$ or $f = 3$.

The next question to investigate is that, given that one has quite a few clusters with $C \geq 5$ and large fraction of the total number of dipoles in these clusters, how many stars is each cluster connected to? These questions is systematically investigated in fig 7 and 8, where the distribution of the number of clusters n_c, normalized by the corresponding total number of cluster C_T, is plotted versus the number of stars N_S that the dipole-clusters gets dipole contributions from. Figure 7 and 8 is for $L = 25$ and $L = 50$, respectively.

For $R = 40, f = 6$ and $L = 25$ stars, which has $C_T \approx 250$ (refer Fig. 3a), three-fourth of the total number of clusters C_T have 5 or more dipoles in a cluster

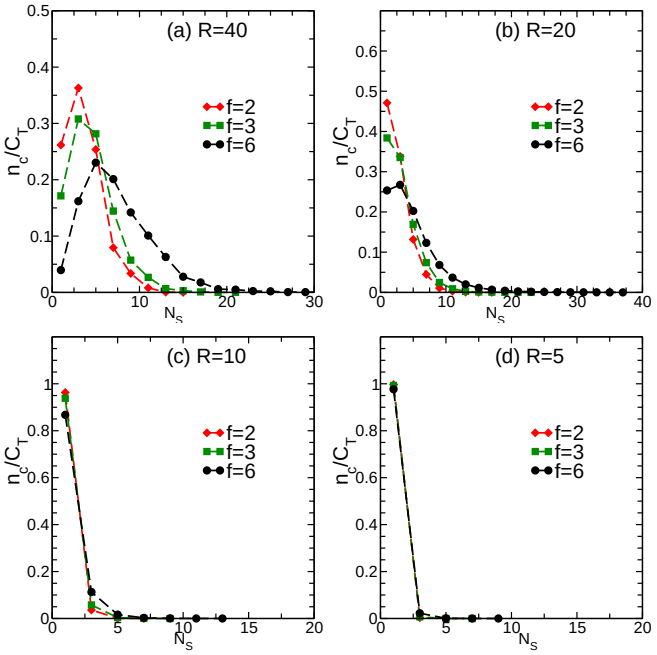

FIG. 7: The plots show the distribution of the number of clusters n_c, normalised by the average of the total number of clusters C_T, versus N_S, the number of stars which contribute dipoles to make up a cluster. Data is for $L = 25$ with 350 stars in simulation box for different values of f, the number of arms in a star with dipoles at arm-tips. For $R = 5, R = 10$, the dipoles do not form clusters with multiple dipoles in cluster and hence has contributions primarily from just one star. In contrast for $R = 40$, each cluster has dipoles from multiple stars. Note that the bin size in the $x-$axis is 2.

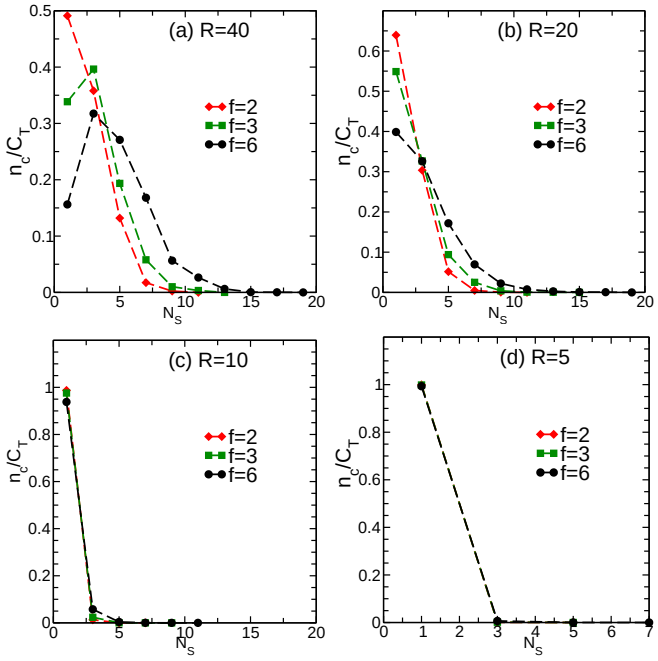

FIG. 8: The plots show, the distribution of the number of clusters n_c, normalised by the average of total number of clusters C_T, are plotted versus N_S, the number of stars which contribute dipoles to make up a cluster. Data is for $L = 50$ with 175 stars in simulation box for different values of f, the number of arms in a star with dipoles at arm-ends. For $R = 10, R = 5$, the dipoles do not form clusters with multiple dipoles, thus $n_C/C_T \approx 1$ for $N_S = 1$. In contrast for $R = 40$, each cluster has dipole contributions from multiple stars.

(refer Fig.4a). Now we can add the values of n_c/C_T for different values of N_S in Fig.7a to see that a predominantly large number of clusters, more than 70%, have contributions from 5 or more stars: the peak of the n_C/C_T distribution is at $N_S = 5, 7$. Moreover, more than 20% of the clusters have $N_S > 10$, i.e., around 50 out of 250 (approximately) clusters have dipole contributions from more than 10 stars! For $f = 2$ and $f = 3$ stars large dipole-clusters are unable to form and hence clusters gets contributions from fewer number of stars N_S compared to the $f = 6$ system. But still 40% of the clusters have dipole contributions from 5 or more stars for $f = 2, f = 3$.

For $R = 20$ with $f = 6$ stars (Fig.7b), where one obtains larger number of smaller clusters, but nearly half of the total number of clusters are connected to more than 5 stars with $N_s \geq 5$ and nearly 75% of the clusters are connected to 3 or more stars. Thus each dipole cluster acts as a node through which different stars are connected by contributing a dipole from one (or more than one) star arm. Other arms of the star could be connected to a different cluster (we systematically investigate this later in the text). Thus there is a possibility of forming a system spanning percolating network of a polymer gel. Even if a percolating network of polymers is not formed for $R = 20$, the star polymers would effectively form very large macromolecules connected through the dipole clusters. There exists few clusters with upto 14 or 16 dipoles per cluster which get contributions from upto $N_S = 14$ stars thus form a very large macromolecule as each star in turn will be connected to other dipole clusters. This can be independently deduced and is consistent with data of Figs. 3a and 4c.

For $R = 20$ with $f = 2, 3$ dipoles per star, one might not get percolating gels or large macromolecules held together by dipole clusters, but stars do get conjoined and form polymers of *effective* larger molecular weight than individual stars. More than half the clusters have contributions from 3 or more stars. For lower values of R, viz, $R = 10$ and $R = 5$ (refer Fig.5a,b), most of the clusters have 1 or 2 dipoles, thereby each cluster has dipole-contributions from 1 or 2 stars: the stars are hardly networked with each other through dipole clusters. Thereby $R = 10, R = 5$ stars do not form a gel-like network of polymers, and this is seen in Fig7c and 7d where more than 90% of clusters are connected to 1 or 2 stars: there are sharp peaks for $N_s = 1$. This result is independent of the value of f, the Coulomb interaction between dipoles R is not enough such that clusters containing many dipoles get aggregated into larger macromole. For $R = 10, f = 6$, there are 10% clusters which are con-

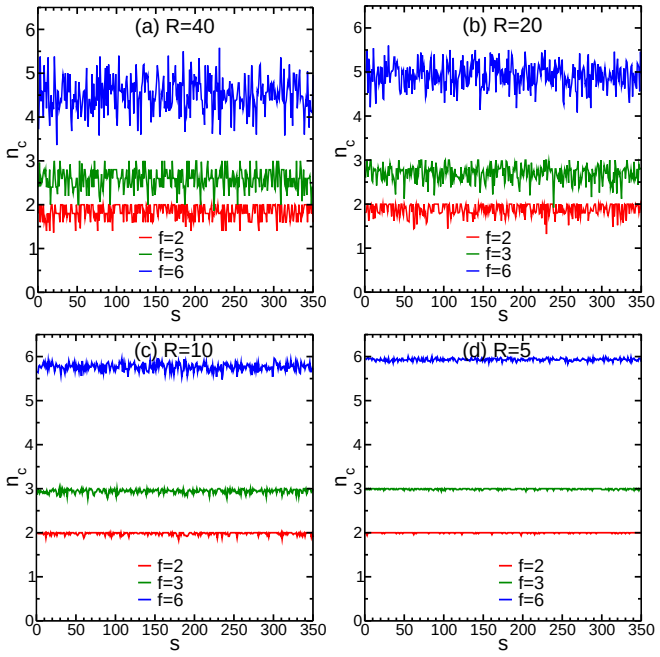

FIG. 9: The subplots show the average number of clusters $n_c(s)$ that each star contributes its dipoles to. The x-axis shows the star index s, the simulation box has 350 stars, and the stars are numbered (indexed) 1 to 350. Subplots (a),(b),(c),(d) correspond to the values of $R = 40, 20, 10, 5$ respectively for case $L = 25$ monomers in a arm. For $R = 5$ and $f = 6$, each dipole is isolated and therefore is in a different cluster with just 1 dipole in cluster. Each star contributes to 6 clusters. However, when $R = 40$ we know that each cluster contains multiple dipoles, thus for $f = 6$ the data shows that 6 different arms contribute dipoles mostly to different clusters. This definitely helps in forming a gel-like network of polymer arms across the box.

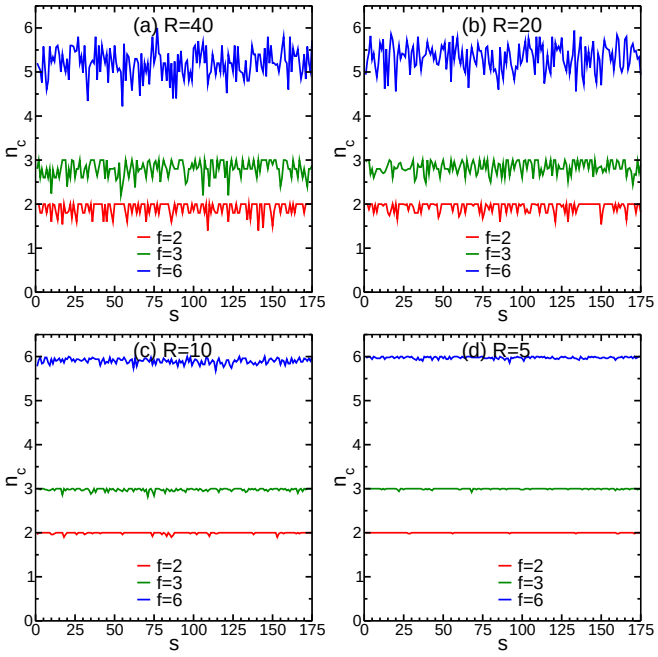

FIG. 10: The subplots show the average number of clusters $n_c(s)$ that each star contributes its dipoles to. The x-axis shows the star index s, the simulation box has 175 stars, and the stars are numbered (indexed) 1 to 175. Subplots (a),(b),(c),(d) correspond to the values of $R = 40, 20, 10, 5$ respectively for case $L = 50$ monomers in a arm.

nected to 2 stars, that is effectively doubling the *effective* molecular weight of these stars which could lead to an effective marginal increase in viscosity.

For $L = 50$ with fewer dipoles in the box, the results and conclusions for $R = 5$ and $R = 10$ stars are not any different from the $L = 25$ stars with $R = 5, 10$ as seen in Fig.8c and d. For $R = 40$ stars the star-polymers get networked when $f = 6$ and $f = 3$ as nearly 50% and 35% of the clusters have dipole contributions from more than 4 stars, respectively. For $f = 6$, one could probably get a percolating gel of stars, but $f = 2$ or $f = 3$, though the stars do get *gelled* through dipole clusters, it is unlikely that the gel will be system spanning/percolating through the system. But one would definitely observe a large increase in effective relaxation-times/viscosity due to the slow dynamics of effectively large macromolecules formed.

For $R = 20, L = 50$, refer Fig.8b, there is very little chance of stars with $f = 2$ or $f = 3$ dipoles to form percolating gel structure of stars. For $f = 6$, the system could form a percolating gel as nearly 30% of the clusters are connected to more than 5 stars, thus 30% of clusters have 5 or more dipoles. This can be independently checked from Fig.5b, moreover, 50% of dipoles are clusters with $C \geq 5$ (ref Fig.5f). At the very least, multiple stars get connected through dipole clusters and form large aggregates of stars. This should lead to significant increase in viscosity through we are do not try to quantify the value of viscosity with the computational resources presently available to us. The other interesting thing to note is that the data for $L = 50, f = 6$ is quantitatively very similar to to the case of $L = 25, f = 3$ for all values of R. As mentioned before the two systems have identical number of dipoles. As we have seen before, there doubling the length of star arms from $L = 25$ to $L = 50$ seems to have no effect on the size distribution of dipoles clusters or the the way clusters get dipole contributions from different stars.

Next we aim to calculate and find out how many clusters does each star contribute arms/dipoles to? Figures 9 and 10 show the average number of clusters n_c (on the y-axis) that each star contributes dipoles to. Data for Figs.9 and 10 is for $L = 25$ and $L = 50$, respectively. A particular star s could contribute to 3, 4 or 5 clusters at different times of the simulation run, thereby we get non-integer values of n_c. For $R = 40, f = 6$ (Fig. 9a) for $L = 25$, each star is connected on an average to between 4 and 5 dipole clusters. This now confirms our previous understanding that this system corresponds to a system spanning star gel-like network. As mentioned before and

shown in figures 7, 70% of clusters have contributions from more than 5 stars. Hence, each star would be contributing multiple arms to such *multiply-connected dipole clusters*, and this would lead to a system-spanning gel like molecular network. With each star connected to clusters with many dipoles, the stars will form a system spanning network of star arms: corresponding to a physical gel. Obviously the energy/stress needed to shear such a polymer gel would be very large compared to a system of *unconnected* star polymers. This will correspond to a large increase in $G^{'}$ and η as seen in rheology experiments of stars with ionomers at star tips.

For lower values of f with $R = 40$, which has fewer large clusters, each arms typically is connected to different dipole-clusters. But it does happen, though rarely, that both the arms with the dipoles of a $f = 2$ star ends up in the same dipole cluster: the average n_c does show values less than 2 for $R = 40$. For almost all values of f,R and L , the value of $n_c(s)$ is close to the value of f for different set of parameters for almost all stars. This indicate that the different arms of stars mostly go to different dipole-clusters and unlikely to aggregate together. For $f = 6$ and $L = 25$ stars, 2 out of 6 different arms do end up in the same cluster, the values of n_c in Fig.9a are between 4 and 5.

However, using our understanding of the previous figures, we must interpret data for $R = 5, R = 10$ very differently from $R = 40, R = 20$. For $R = 10, 5$, we know that there are no large clusters and each dipole is nearly free and isolated, so of course each star is shown to contribute each arm to different clusters. On the other hand for $R = 40, R = 20$, we know that a very large proportion of clusters are clusters with 5 or more dipoles, so most of the star arms connect to such multi-dipole clusters. As mentioned before, this indicates that each star will be multiply connected with different stars through an average of 4 different dipole clusters, and sometimes 2 arms from the same star can land up in the same dipole cluster. A few arms of stars will of course be free and not connected to clusters. Note that for $L = 50$ with $R = 40, R = 20$ and $f = 6$, the values of n_c is larger than that for the corresponding $L = 25$ studies. Our understanding is that the $L = 50$ stars have smaller number of clusters, and it is more possible for a star arm to end up as a free arm with cluster size $C = 1$.

IV. DISCUSSION

To conclude, we establish by molecular dynamics simulation of a melt of star polymers with dipoles at the tip of star-arms that for values of effective charge $qe = 0.57e$ and $qe = 0.81e$ ($R = 20$ and $R = 40$, respectively at $T = 300K$) of effective charges we get a high degree of network formation through the formation of dipole clusters. Typically, each arm of a star is connected to a different dipole cluster. Each dipole cluster for $f = 6$ has contributions from many stars so the system should be nearly a percolating gel. A small fraction of arms may remain free for stars with just 2 or 3 dipoles per star. Given that the energy per dipole is quite high compared to k_BT, it would be difficult to break the clusters. Data suggests that it is likely to be a percolating gel for $R = 40$, but could be a non-percolating gel for $R = 20$ especially for lower values of f. For $f = 2, f = 3$, the network of stars will result in effective macomolecules of large molecular weight. Such network formation of stars through dipole clusters should lead to a large increase in viscosity when the star-polymer melt is sheared. The network formation or physical gelation resulting in an increase in viscosity of the melt is more for $f = 6$ stars compared to $f = 2, f = 3$ stars, in tune with experimental observations.

For lower values of R, i.e. $R = 10$ and $R = 5$, the dipoles at star arms do not aggregate sufficiently to form a physical gel. However, there is some clustering resulting in effective increase of molecular weight of networked stars for $R = 10$. The average energy per dipole is $5k_BT$ at $k_BT = 1$ for $R = 5$, that is same as the energy of an isolated dipole showing the effective attractive interaction between dipoles is negligible. If the diameter of monomers is smaller than $1nm$, one could get clusters at significantly lower values of qe. This is because the interaction energy between 2 interacting dipoles should increase as oppositely charged monomers can approach each other to smaller distances.

The other interesting observation is that doubling the length of star arms has no effect in the distribution of size of dipole clusters, if we keep the uncharged monomer density as well as the dipole density the fixed. So it is more useful to have telechelic stars with relatively shorter arms with large f, if one wants to increase effective viscosity of a polymer through this mechanism.

Finally, because we have modelled dipoles by explicit charges instead of effective dipolar interaction, the arrangement of dipoles in the dipole clusters of our simulations is very different from previously known studies [23–25]. For $R = 40$, dipoles arrange themselves antiparallel to each other in a row and form elongated aggregates as that is the low energy configuration compared to the dipoles lining up with every dipole moment approximately pointing in the same direction [23–25]. It could be relevant to revisit current understandings regarding structure formation in dipolar fluids.

We would like to acknowledge useful discussions with Ashish Lele and Arijit Bhattacharyay. We would also like to acknowledge computing facilities procured by DST-SERB grant no. EMR/2015/000018, and the Yuva cluster of CDAC-Pune.

[1] Amruta Kulkarni, Ashish Lele, Swaminathan Sivaram, P. R. Rajamohanan, Sachin Velankar, Apratim Chatterji, Macromolecules, **48**, 6580 (2015).

[2] Charlotte K. Williams, Chem. Soc. Rev., **36**, 15731580 (2007).
[3] Alfonso Rodriguez-Galan, Lourdes Franco and Jordi Puiggali, Polymers, Polymers, **3**, 65-99 (2011).
[4] Xiaoyan Li, Huajian Gao, Nature Materials **15**, 373374 (2016).
[5] R. Dolog, R.A. Weiss, Macromolecules, **46**, 78457852 (2013).
[6] L.J. Fetters, W.W. Graessley, Nikos Hadjichristidis, Andrea D. Kiss, Dale S. Pearson, and Lawrence B. Younghouse, Macromolecules, **21**, 1644 (1988).
[7] E. van Ruymbeke, D. Vlassopulos, M. Mierzwa, T. Pakula, D. Charalabidis, M. Pitsikalis, and N. Hadjichristidis, Macromolecules, **43**, 4401 (2010).
[8] Federica Lo Verso, Christos N. Likos, Polymer, **49** 1425 (2008).
[9] Federica Lo Verso, Christos N. Likos, Christian Mayer, and Hartmut Löwen, Phys.Rev. Lett.,**96**, 187802 (2006).
[10] B. Capone, I. Coluzza, R. Blaak, F. Lo Verso, and C. N. Likos, New J. of Phys. **15** 095002 (2013).
[11] R. Blaak, S. Lehmann, and C. N. Likos, Macromolecules, **41**, 4452-4458 (2008).
[12] B. Capone, I. Coluzza, F. Lo Verso, C. N. Likos, and R. Blaak, Phys. Rev. Lett., **109**, 238301 (2012).
[13] Sanat K. Kumar, A.Z. Panagiotopoulos, Phys. Rev. Lett., **82** 5060 (1999).
[14] Sanat K. Kumar, J.F. Douglas, Phys. Rev. Lett., **87** 188301 (2001).
[15] Pablo I. Hurtado, Ludovic Berthier, and Walter Kob, Phys. Rev. Lett. **98**, 135503 (2007).
[16] Jin Suk Myung, Roland G. Winkler, and Gerhard Gompper, J.Chem. Phys., **143**, 243117 (2015).
[17] Ro, A. J.; Huang, S. J.; Weiss, R. A. Polymer 2008, 49, 422431.
[18] Ro, A. J.; Huang, S. J.; Weiss, R. A. Polymer 2009, 50, 11341143.
[19] A. Eisenberg, Macromolecules, **4**, pp 125128, 1971.
[20] Mark J. Stevens and Gary S. Grest, Phys. Rev. Lett., **72**, 3686 (1994).
[21] J. J. Weis and D. Levesque, Phys. Rev. Lett., **71**, 2729 (1993).
[22] J. M. Tavares, J. J. Weis, and M. M. Telo da Gama, Phys. Rev. E, **59** 4388 (1999).
[23] Mark J. Stevens and Gary S. Grest, Phys. Rev. E, **51** 5976 (1995).
[24] Mark J. Stevens and Gary S. Grest, Phys. Rev. E, **51** 5962 (1995).
[25] D. Levesque and J. J.Weis, Phys. Rev. E, **49** 5131 (1994).
[26] Sunil P. Singh, Apratim Chatterji, Gerhard Gompper and Roland G. Winkler, Macromolecules, **46**, 8026 (2013).
[27] D.A. Fedosov, S.P. Singh, A. Chatterji, R.G. Winkler, G.Gompper, Soft Matter, **8**, 4109- 4120, (2012)
[28] S.P.Singh, D.A. Fedosov, A. Chatterji, R.G. Winkler,G. Gompper,J. of Phys.: Condens. Matt., 24, 464103, (2012).
[29] S. Plimpton, J. Comp. Phys, **117**, 1-19 (1995); http://lammps.sandia.gov/ .
[30] Markus Deserno and Christian Holm, J. Chem. Phys., **109**,7678 (1998).
[31] Markus Deserno and Christian Holm, J. Chem. Phys., **109**,7694 (1998).
[32] Intermolecular and Surface Forces, Jacob N. Israelachvili, Academic Press (2011).
99